



Received: April 16, 2025
Revised: May 26, 2025
Accepted: June 23, 2025

Corresponding Author:
Udom Thongudomporn,
Orthodontic Section, Department
of Preventive Dentistry, Faculty of
Dentistry, Prince of Songkla University,
Songkhla 90110, Thailand
E-mail: udom.t@psu.ac.th

Effects of Light Intensity and Color from Softbox Light Sources on 3D Facial Measurements Using a Structured-Light 3D Facial Scanner

Bussara Pongsermsuk, Udom Thongudomporn

Orthodontic Section, Department of Preventive Dentistry, Faculty of Dentistry,
Prince of Songkla University, Thailand

Abstract

Objectives: This study evaluated the effects of light intensity and color on facial dimensions measured along three axes (X, Y, and Z) using a structured-light 3D facial scanner.

Methods: Forty-seven adults (mean age 25.7 ± 3.4 years) underwent facial scanning under two light intensities (500 and 700 lux) and two light colors (daylight and cool white) generated from a softbox photography lighting setup. The scans were performed in a room illuminated with ambient daylight-color LED at 300 lux without external light interference. Facial measurements were analyzed using Dolphin Imaging Software. Two-way repeated measures ANOVA was used to assess the effects of light intensity, light color, and their interactions on facial measurements. Statistical significance was set at $p < 0.05$.

Results: Light intensity had no significant effect on 3D facial measurements ($p > 0.05$). However, light color significantly influenced upper lip anterior-true vertical line through the alar base (ULA-TVL) and lower lip anterior-true vertical line through the alar base (LLA-TVL) measurements along the Z axis ($p < 0.05$), with greater values recorded under daylight compared to cool white. No significant interaction effect between light intensity and light color was observed ($p > 0.05$).

Conclusions: Light color influences upper and lower lip protrusion measurements in 3D facial scanning with a structured-light 3D facial scanner, whereas light intensity does not. Standardizing light color is recommended for consistent measurements.

Keywords: face, lighting, photography, 3D imaging

Introduction

Facial 3D scanning is increasingly used in various fields of dentistry,⁽¹⁻³⁾ especially in complex cases where facial soft tissue correction is an essential part of treatment planning.⁽⁴⁾ The advantage of a 3D facial scan lies in its capacity to capture the entire face in three dimensions without exposing the subject to radiation while also minimizing angular errors. This technology enables precise quantification of linear, angular, and volume changes in facial regions,⁽⁵⁾ the evaluation of facial deformities, and superimposition for assessing treatment outcomes in fields such as orthodontics, maxillofacial surgery, and prosthodontics.⁽⁴⁾ These capabilities surpass those of direct measurement with a vernier caliper, which offers crude measurements of a complex 3D morphology.⁽⁶⁾

Studies have assessed the accuracy of various types of 3D facial scanner technologies including stereophotogrammetry,^(1,7,8) monoscopic photogrammetry,^(2,8,9) 3D laser scanners,^(3,9,10) structured-light scanners,^(1-3,11,12) and infrared scanners.^(2,3,11,12) No significant difference has been found between structured-light scanners and stereophotogrammetry,⁽¹⁾ but structured-light scanners have been reported to be more accurate than 3D laser⁽³⁾ and infrared scanners.^(2,3,11,12) In contrast, monoscopic photogrammetry has been found to be less accurate than stereophotogrammetry⁽⁸⁾ but more accurate than 3D laser scanning.⁽⁹⁾ These findings suggest that structured-light scanners may offer the highest accuracy among the various types of scanners.

Factors that reduce scanner accuracy include the complexity of the patient's facial shape and surface conditions, such as concavities and undercut areas,⁽¹⁾ as well as lighting conditions during scanning.⁽¹⁰⁾ Ambient light can decrease the intensity of the light projected by scanners, leading to degraded reconstruction quality⁽¹³⁾ and inaccurate coordinate measurements.⁽¹⁴⁾ Moreover, using only overhead ambient lighting in a room has been reported to cause images to have a greenish tint.⁽¹⁵⁾ Additionally, a laboratory experiment found that the color of the light source (e.g., daylight, cool white, or dark night) can influence the range accuracy of certain colors on a 24-color patch chart.⁽¹⁶⁾

Medical imaging requires proper and sufficient illumination of the surface. Overhead ambient lighting alone may cause uneven shadows and reduce image detail capture around cervical areas, especially in subjects with

dark skin tones. Using additional hard light sources, such as ring flashes, is not recommended, as they produce flat images with inaccurate details and colors of the actual face.^(15,17-22) Studies have recommended positioning at least two light sources at a 45-degree angle to both the subject and the camera with the light passing through a diffusion layer to reduce light harshness and hard shadows. This can be achieved using a softbox or lighting umbrella.⁽¹⁷⁻²¹⁾

Two key light parameters commonly considered in imaging are light intensity and light color. Light intensity, measured in lumens per square meter (Lm/m^2) or lux⁽¹⁴⁾ represents the amount of light emitted onto a surface, while light color ranges from warm yellow to cool blue. The effect of light intensity and color during facial scanning with a structured-light facial scanner on the accuracy of obtained measurements remains unclear. This study aimed to examine the effect of two different light intensities and two different colors, projected from a softbox light source setup, on distance measurements along the X, Y, and Z axes during a 3D facial scan. The null hypothesis was that distance measurements obtained from a structured-light facial scanner under different light intensities and colors would not differ significantly.

Material and Methods

Sample size

This study was approved by the Faculty of Dentistry, Prince of Songkla University Ethics Committee (EC-6704-022). All procedures were conducted in accordance with relevant laws and ethical guidelines. The sample size was determined based on a previous study investigating the accuracy and precision of 3D images obtained from a structured-light facial 3D scanner.⁽²³⁾ The sample size calculation was performed using G*Power software (version 3.1.9.2), with parameters set at $\alpha=0.05$, power=0.9, and effect size=0.4.⁽²³⁾ The minimum required sample size was 44.

The inclusion criteria were subjects aged 18-30 years with normal physical health, a visually normal facial morphology with balanced proportions and symmetry, and no visible abnormalities or deformities. Exclusion criteria included craniofacial anomalies, a history of craniofacial trauma or facial surgery, excessive facial hair that might obscure anatomical landmarks, facial scars or birthmarks,

ongoing orthodontic treatment, and an inability to comply with the experimental protocol. The study procedure was explained to each volunteer, privacy rights were observed, and written informed consent was obtained.

Subject preparation and scanning process

Subjects were asked to remove makeup, accessories, and excessive facial hair. Hair was tied back, and a headband was used if necessary. A black apron was worn to cover their clothing. Following previous studies^(8,12,24) fifteen anatomical landmarks (Table 1) were marked on each the subject's facial skin using edible marker by a single operator (Figure 1). For each subject, landmarks were placed once to minimize potential marking errors.

Subjects were seated 30 cm from the facial 3D scanner in a natural head position. They were instructed to slowly rotate their heads up and down, gradually reducing the range of motion until they achieved a balanced position. Once positioned, they looked into a mirror placed 200 cm away at eye level, followed by an assessment from the researcher to ensure a natural appearance. Subjects were then asked to say "Emma" to relax their lips before gently bringing their teeth into maximum intercuspation with light occlusal contact, the same position used for routine lateral cephalometric radiographs. Their eyes remained open and their ears were included in all scans.

3D facial scans were performed in a room illuminated by ambient overhead daylight-colored LED lighting at 300 lux, with no external light interference. Additional lighting was provided by two softbox light sources placed 150 cm away from the subject at a 45-degree angle relative to both the facial 3D scanner and the subject. This setup produced combinations of either 500 lux or 700 lux intensity. These values were selected based on the recommendations of the European Standard EN-12464: 2011⁽²⁵⁾ which state that acceptable illumination levels for physicians' examination rooms should range between 500 and 1,000 lux. At each light intensity, two lighting color temperatures, daylight and cool white, were tested.

Before each scan, light intensity was measured using a lux meter (DIGICON LX-50, Digicon Inc, Japan) to ensure accuracy. Subject were allowed to rest for at least 30 seconds with the lights turned off to reduce eye strain between scans, after which the natural head position setting method was repeated. A structured-light facial 3D scanner (Accu3DX Co., Ltd) was used, and the scanning sequence followed four conditions: 500 lux+daylight; 500 lux+cool white; 700 lux+daylight; and 700 lux+cool white. Each lighting condition was scanned only once per subject.

The scanning process for each subject began with a front view, followed by the right, left, and neck views.

Table 1: Facial landmarks, abbreviations, and definitions.

Anthropometry point	Abbreviation	Definition
Nasion	N	The midpoint on the soft tissue contour of the base of the nasal root at the level of the frontonasal suture
Alar contour	AcL, AcR	The lowest point of alar base (left and right sides)
Pronasale	Pmn	The most anterior midpoint of nasal tip
Subnasale	Sn	The midpoint on the nasolabial soft tissue contour between the columella crest and the upper lip
Cheilion	ChL, ChR	The outermost point of vermilion border (left and right sides)
Labiale superioris	Ls	Midpoint of the upper vermilion line (upper vermilion border)
Stomion	Sto	The middle contact point of upper and lower lips (in competent lips)
Stomion superius	Sts	The most inferior midpoint of the vermilion border of the upper lip (in incompetent lips)
Stomion inferius	Sti	The most superior midpoint of the vermilion border of the lower lip (in incompetent lips)
Labiale inferioris	Li	Midpoint of the lower vermilion line (lower vermilion border)
Supramentale	Sm	The most posterior midpoint on the labiomental soft tissue contour that defines the border between the lower lip and the chin
Pogonion	Pg	The most anterior midpoint of the chin
Gnathion	Gn	The most inferior midpoint on the soft tissue contour of the chin
Upper lip anterior	ULA	The most anterior midpoint on upper lip
Lower lip anterior	LLA	The most anterior midpoint on lower lip

A white mesh visible-spectrum projection pattern was projected onto the face and captured from four angles by an operator with experience in facial scanning, having worked on more than 20 cases. The scanner was calibrated before each scanning session.

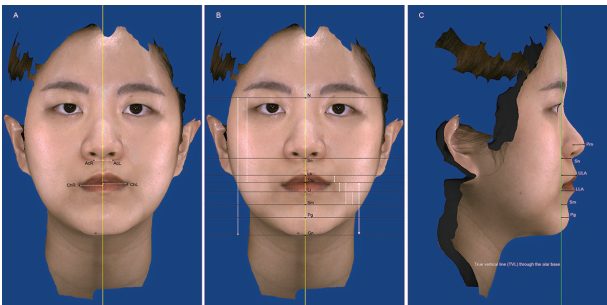


Figure1: Facial landmarks and measurements used in the study. (A), X axis: (B), Y axis: (C), Z axis.

3D facial measurement

The scanned facial images, saved as OBJ files, were analyzed using Dolphin Imaging 11.9 (Dolphin Imaging Systems LLC). Measurement variables in three axes (Figure 1), adapted from previous studies^(24,26,27) are presented Table 2. The X-axis represented width, running parallel to the interpupillary line; the Y-axis represented length, running perpendicular to the X-axis and passing through the facial midline; and the Z-axis represents depth in the anteroposterior direction, running perpendicular to the true vertical line aligned with Earth's gravity and perpendicular to the ground.

To assess intra-examiner reliability, all measurements were repeated twice on ten randomly selected subjects, with each measurement taken two weeks apart.

Statistical analysis

Statistical analysis was performed using SPSS software (Statistical Package for the Social Sciences, version 29.0.1.0, IBM Corp). The Shapiro-Wilk test was used to assess the normality of data distribution. For non-normally distributed data, logarithmic transformation was applied to achieve normality. Two-way repeated measures ANOVA was conducted to analyze variance. Intra-examiner reliability was evaluated using the intraclass correlation coefficient (ICC). Significance was set at $p<0.05$.

Results

Forty-seven healthy volunteers participated in the study. The mean age was 25.7 ± 3.4 years with 33 females (70.2%) and 14 males (29.8%). Descriptive statistics, including the mean and standard deviation, are presented in Table 3. The ICC values for the X, Y, and Z axes ranged from 0.985–0.999, 0.929–0.999, and 0.986–0.999, respectively, indicating excellent reliability for every lighting condition.

Table 4 presents the results of the two-way analysis of variance. Light intensity (500 lux vs. 700 lux) did not significantly affect the measured distances in any of the three dimensions ($p>0.05$). However, light color significantly influenced the distances of the upper lip anterior-true vertical line through the alar base (ULA-TVL) and lower lip anterior-true vertical line through the alar base (LLA-TVL) along the Z axis ($p<0.05$), while distances along the X and Y axes remained unaffected ($p>0.05$). ULA-TVL and LLA-TVL measurements were significantly greater under daylight conditions than under cool white light, with mean differences of 0.45 ± 0.19 mm and 0.37 ± 0.15 mm, respectively. No significant interaction

Table 2: 3D distance measurements in X, Y, and Z axes in millimeters.

X axis	Y axis	Z axis
AcL-AcR	N-Gn	Sn-Prn
ChL-ChR	N-Sto	Sn-TVL through the alar base
	Ls-Sto	ULA-TVL through the alar base
	Sto-Sm	LLA-TVL through the alar base
	Sto-Li	Sm-TVL through the alar base
	Li-Sm	Pg-TVL through the alar base
	Sto-Gn	

True vertical line (TVL) through the alar base was measured on the right side.

between light intensity and color was observed in any of the three dimensions ($p>0.05$).

Discussion

This study found that increasing light intensity from 500 lux to 700 lux did not affect facial scan measurements along the X, Y, or Z axes. However, changing light color from daylight to cool white resulted in significant deviations in lip protrusion measurements along the Z axis. No significant interaction was observed between light intensity and light color.

A previous study reported that increasing light intensity enhanced the completion of 3D facial scans, leading to improved measurement accuracy, particularly along the Z axis, which is often less precise due to insufficient light reaching the deeper surfaces.⁽³⁾ However, that study used a polyacrylic model, whereas the present study focused on scanning human skin. Building on their findings, it was demonstrated that light intensity of 500 lux and 700 lux did not cause deviations in measurements along any axis, suggesting that both intensities are interchangeable in practical applications.

A change in light color during the scanning affected the upper and lower lip measurements along the Z axis (depth dimension) but did not influence other distance

measurements. Daylight color resulted in greater distances for these two parameters compared to cool white color, which could be attributed to several factors.

First, daylight color provides higher contrast and clarity,⁽²⁸⁾ making the edges of the lips more distinct that leading to more precise measurements. In contrast, cool white light may not offer the same level of contrast, potentially causing slight blurring at the lip edges, which could shorten the perceived lip protrusion.

Second, lip color varies from light pink to brown, which distinguishes it from other facial skin areas. This suggests that light color may have a greater impact on regions with these hues compared to skin-toned areas.

Our findings contrast with a previous laboratory study⁽¹⁶⁾ which projected different light colors onto a Macbeth ColorChecker chart containing 24 colors and scanned it using a structured-light scanner. That study found that red tones on the chart exhibited less deviation in image capture compared to light and dark skin tones. However, it is important to note that light pink to brown hues – resembling natural lip color - were not represented on the chart. Additionally, the absorption and scattering properties of the color chart may differ from those of human skin.

Lastly, the absence of a significant interaction effect

Table 3: Descriptive statistics for measurements under different light conditions in millimeters.

Measurements	Mean \pm SD			
	500 lux Daylight	500 lux Cool white	700 lux Daylight	700 lux Cool white
X axis				
AcL-AcR	19.18 \pm 0.27	19.29 \pm 0.27	19.26 \pm 0.26	19.13 \pm 0.24
ChL-ChR	46.52 \pm 3.46	46.62 \pm 3.50	46.56 \pm 3.73	46.78 \pm 3.49
Y axis				
N-Gn	112.90 \pm 5.42	112.90 \pm 5.51	113.01 \pm 5.41	113.19 \pm 5.48
N-Sto	74.58 \pm 3.75	74.71 \pm 3.76	74.99 \pm 3.77	74.72 \pm 3.90
Sto-Gn	38.08 \pm 4.20	38.00 \pm 4.25	38.10 \pm 4.29	38.15 \pm 4.33
Sto-Sm	16.70 \pm 2.21	16.64 \pm 2.20	16.75 \pm 2.22	16.67 \pm 2.27
Li-Sm	5.73 \pm 1.96	5.75 \pm 2.02	5.81 \pm 1.79	5.76 \pm 1.98
Ls-Sto	7.59 \pm 1.32	7.56 \pm 1.33	7.47 \pm 1.30	7.48 \pm 1.22
Sto-Li	10.86 \pm 1.78	10.78 \pm 1.82	10.87 \pm 1.64	10.82 \pm 1.76
Z axis				
Sn-Prn	12.19 \pm 1.81	12.18 \pm 1.71	12.29 \pm 1.79	12.26 \pm 1.72
Sn-TVL	8.65 \pm 2.27	8.58 \pm 2.24	8.68 \pm 2.41	8.60 \pm 2.12
ULA-TVL	13.18 \pm 2.58	12.78 \pm 2.67	13.28 \pm 3.08	12.79 \pm 2.59
LLA-TVL	11.57 \pm 2.94	11.27 \pm 2.97	11.66 \pm 3.06	11.21 \pm 2.90
Sm-TVL	4.91 \pm 3.52	4.64 \pm 3.47	4.88 \pm 3.75	4.76 \pm 3.55
Pg-TVL	6.52 \pm 3.84	6.24 \pm 3.93	6.46 \pm 4.25	6.34 \pm 4.00

Table 4: Summary of the two-way repeated measures ANOVA results for the measurements.

Light	Measurements	Sum of squares	Degree of freedom	Mean square	F-value	p-value
Intensity	X axis					
	AcL-AcR	0.07	1	0.07	0.24	0.63
	ChL-ChR	0.44	1	0.44	0.25	0.62
	Y axis					
	N-Gn	0.00	1	0.00	2.96	0.09
	N-Sto	2.13	1	2.13	3.48	0.07
	Sto-Gn	0.31	1	0.31	0.57	0.46
	Sto-Sm	0.00	1	0.00	1.01	0.31
	Li-Sm	0.10	1	0.10	0.65	0.44
	Ls-Sto	0.42	1	0.42	1.34	0.25
	Sto-Li	0.03	1	0.03	0.06	0.81
	Z axis					
	Sn-Prn	0.37	1	0.37	1.48	0.23
	Sn-TVL	0.02	1	0.02	0.02	0.88
Color	ULA-TVL	0.12	1	0.12	0.06	0.82
	LLA-TVL	0.01	1	0.01	0.01	0.93
	Sm-TVL	0.02	1	0.02	0.69	0.41
	Pg-TVL	0.02	1	0.02	1.14	0.29
	X axis					
	AcL-AcR	0.00	1	0.00	0.00	0.96
	ChL-ChR	1.31	1	1.31	0.70	0.41
	Y axis					
	N-Gn	0.00	1	0.00	0.24	0.63
	N-Sto	0.23	1	0.23	0.33	0.57
	Sto-Gn	0.01	1	0.01	0.01	0.91
	Sto-Sm	0.00	1	0.00	0.02	0.88
	Li-Sm	0.01	1	0.01	0.05	0.83
	Ls-Sto	0.00	1	0.00	1.00	0.91
	Sto-Li	0.18	1	0.18	0.41	0.53
	Z axis					
	Sn-Prn	0.02	1	0.02	0.08	0.78
	Sn-TVL	0.28	1	0.28	0.39	0.54
	ULA-TVL	9.43	1	9.43	5.58	0.02*
	LLA-TVL	6.44	1	6.44	6.12	0.02*
	Sm-TVL	0.03	1	0.03	2.82	0.10
	Pg-TVL	0.03	1	0.03	1.15	0.29
Intensity and color interaction	X axis					
	AcL-AcR	0.68	1	0.68	2.76	0.10
	ChL-ChR	0.16	1	0.16	0.10	0.76
	Y axis					
	N-Gn	0.00	1	0.00	2.11	0.15
	N-Sto	1.88	1	1.88	2.72	0.11
	Sto-Gn	0.20	1	0.20	0.48	0.49
	Sto-Sm	0.00	1	0.00	1.64	0.21
	Li-Sm	0.05	1	0.05	0.17	0.69
	Ls-Sto	0.02	1	0.02	1.00	0.75
	Sto-Li	0.01	1	0.01	0.03	0.87
	Z axis					
	Sn-Prn	0.00	1	0.00	0.02	0.88
	Sn-TVL	0.00	1	0.00	0.00	0.97
	ULA-TVL	0.11	1	0.11	0.06	0.81
	LLA-TVL	0.22	1	0.22	0.21	0.65
	Sm-TVL	0.00	1	0.00	0.04	0.85
	Pg-TVL	0.00	1	0.00	0.14	0.72

* Statistical significance at $p < 0.05$.

between light color and light intensity suggests that the influence of light color on the facial measurements was independent of light intensity.

This study was conducted in a sealed room, eliminating external light interference. Natural light can affect image color, as its characteristics vary throughout the day, with midday light tends to have a bluer tint, while morning and evening light appear warmer.^(9,29) Additionally, the light intensities and colors tested in this study are commonly found in commercially available light bulbs. This enhances the practical applicability of the findings, making them relevant for real-world settings.

This study has some limitations. The findings are specific to individuals with morphologically normal faces and skin tones ranging from light-medium to tan, typical of Asian skin tones. As a result, these findings cannot be generalized to individuals with other skin tones. No comparisons were made with other types of 3D facial scanners or different brands of the same scanner type. While the same light bulbs were used and the light intensity was calibrated with a lux meter throughout the study, light color calibration was not performed. Using a light color meter to measure color temperature could have ensured greater consistency in light color conditions. This study lacked an ambient light-only control group, which could have shown how the measurements differed from those taken under additional lighting conditions. Additionally, the scanning sequence was not randomized. This may have introduced potential order effects related to subject adaptation, fatigue, or varying responses to lighting exposure during repeated scans.

Furthermore, this study focused on precision (reproducibility across conditions) in measurements under different light intensities and colors rather than on measurement accuracy (closeness to truth). Evaluating accuracy would typically require a reference model as a gold standard, as human skin exhibits natural variations due to melanin, blood vessels, and oiliness. However, examining the effect of light intensity and color on an artificial model may not fully translate to human skin, given the differences in light absorption and scattering properties.

The clinical implications of this study suggest that when using a structured-light scanner for 3D facial scanning of the same subject, an additional light intensity of either 500 lux or 700 lux can be interchangeable. To ensure

consistency, it is recommended to use the same light color throughout the scanning process. Although it was not conclusive from this study, daylight color may be more appropriate, as previous studies^(15,20) have indicated that it provides neutral lighting, minimizing unwanted yellow or green tints in the images.

Conclusions

- A light intensity of 500 lux or 700 lux did not affect any of the three-dimensional measurements obtained from a structured-light 3D facial scanner.

- Light color variations during 3D facial scanning influenced upper and lower lip protrusions along the Z axis.

Acknowledgments

The authors sincerely appreciate the financial support provided by the Graduate School and the Faculty of Dentistry, Prince of Songkla University.

References

1. Zhao YJ, Xiong YX, Wang Y. Three-dimensional accuracy of facial scan for facial deformities in clinics: a new evaluation method for facial scanner accuracy. *PLoS One*. 2017;12(1):e0169402.
2. Tsuchida Y, Shiozawa M, Handa K, Takahashi H, Nikawa H. Comparison of the accuracy of different handheld-type scanners in three-dimensional facial image recognition. *J Prosthodont Res*. 2023;67(2):222-30.
3. Amornvit P, Sanohkan S. The accuracy of digital face scans obtained from 3D scanners: an *in vitro* study. *Int J Environ Res Public Health*. 2019;16(24):5061.
4. Hajeer MY, Millett D, Ayoub A, Siebert J. Applications of 3D imaging in orthodontics: Part 1. *J Orthod*. 2004;31:62-70.
5. Pellitteri F, Scisciola F, Cremonini F, Baciliero M, Lombardo L. Accuracy of 3D facial scans: a comparison of three different scanning system in an *in vivo* study. *Prog Orthod*. 2023;24(1):44.
6. Weinberg SM. 3D stereophotogrammetry versus traditional craniofacial anthropometry: Comparing measurements from the 3D facial norms database to Farkas's North American norms. *Am J Orthod Dentofacial Orthop*. 2019;155(5):693-701.
7. Wong JY, Oh AK, Ohta E, Hunt AT, Rogers GF, Mulliken JB, *et al*. Validity and reliability of craniofacial anthropometric measurement of 3D digital photogrammetric images. *Cleft Palate Craniofac J*. 2008;45(3):232-9.
8. Staller S, Anigbo J, Stewart K, Dutra V, Turkkahraman H. Precision and accuracy assessment of single and multi-camera three-dimensional photogrammetry compared with

- direct anthropometry. *Angle Orthod.* 2022;92(5):635-41.
9. Ayaz I, Shaheen E, Aly M, Shujaat S, Gallo G, Coucke W, *et al.* Accuracy and reliability of 2-dimensional photography versus 3-dimensional soft tissue imaging. *Imaging Sci Dent.* 2020;50(1):15-22.
 10. Joe PS, Ito Y, Shih AM, Oestenstad RK, Lungu CT. Comparison of a novel surface laser scanning anthropometric technique to traditional methods for facial parameter measurements. *J Occup Environ Hyg.* 2012;9(2):81-8.
 11. Koban KC, Perko P, Etzel L, Li Z, Schenck TL, Giunta RE. Validation of two handheld devices against a non-portable three-dimensional surface scanner and assessment of potential use for intraoperative facial imaging. *J Plast Reconstr Aesthet Surg.* 2020;73(1):141-8.
 12. Koban KC, Perko P, Li Z, Xu Y, Giunta RE, Alfertshofer MG, *et al.* 3D Anthropometric Facial Imaging-a comparison of different 3D scanners. *Facial Plast Surg Clin North Am.* 2022;30(2):149-58.
 13. Thongma-Eng P, Amornvit P, Silthampitag P, Rokaya D, Pisitanusorn A. Effect of ambient lights on the accuracy of a 3-dimensional optical scanner for face scans: an *in vitro* study. *J Healthc Eng.* 2022;2022(1):2637078.
 14. Katsioloudis PJ, Jones M. Effects of light intensity on spatial visualization ability. *J Technol Stud.* 2017;43(1):2-13.
 15. Chen BR, Poon E, Alam M. Photography in dermatologic surgery: selection of an appropriate lighting solution for a particular clinical application. *Dermatol Surg.* 2018;44(1):106-14.
 16. Voisin S, Fougou S, Truchetet F, Page D, Abidi M. Study of ambient light influence for three-dimensional scanners based on structured light. *Opt Eng.* 2007;46(3):30502-3.
 17. Swamy RS, Most SP. Pre-and postoperative portrait photography: standardized photos for various procedures. *Facial Plast Surg Clin North Am.* 2010;18(2):245-52.
 18. Daniel RK, Hodgson J, Lambros VS. Rhinoplasty: the light reflexes. *Plast Reconstr Surg.* 1990;85(6):859-66.
 19. Fernández-Pellón R, Saghir M, Jaber A, Apaydin F. Which lighting option is the best for photography in rhinoplasty?. *Facial Plast Surg.* 2021;37(05):657-65.
 20. Khavkin J, Ellis D. Standardized photography for skin surface. *Facial Plast Surg Clin North Am.* 2011;19(2):241-6.
 21. Galdino GM, DaSilva D, Gunter JP. Digital photography for rhinoplasty. *Plast Reconstr Surg.* 2002;109(4):1421-34.
 22. Shah AR, Hamilton GS, Dayan SH. Pitfalls of photography for facial resurfacing and rejuvenation procedures. *Facial Plast Surg.* 2005;21(2):154-61.
 23. Kim SH, Jung WY, Seo YJ, Kim KA, Park KH, Park YG. Accuracy and precision of integumental linear dimensions in a three-dimensional facial imaging system. *Korean J Orthod.* 2015;45(3):105-12.
 24. Chalearnthongtakul S, Arunjarosensuk S, Kaboosaya B, Dhaneuan K, Tunwatatanapong B, Pimkhaokham A. The accuracy and precision of twelve-angle camera facial scan system for measurement of facial soft tissue. *J Dent Assoc Thai.* 2023;73(2):145-52.
 25. Comité Européen de Normalisation (CEN). Light and lighting- Lighting of work places- Part 1: Indoor work places. EN 12464-1. 2011:33-90.
 26. Farkas LG, Thompson B, Phillips JH, Katic MJ, Cornfoot ML. Comparison of anthropometric and cephalometric measurements of the adult face. *J Craniofac Surg.* 1999;10(1):18-25.
 27. Swennen GR, Schutyser FA, Hausamen JE. Three-dimensional cephalometry: a color atlas and manual: Springer Science & Business Media; 2005:260-70.
 28. DeLaney W, Hughes P, McNelis J, Sarver J, Soules T. An examination of visual clarity with high color rendering fluorescent light sources. *Leukos.* 1978;7(2):74-84.
 29. Jakowenko J. Clinical photography. *J Telemed Telecare.* 2009;15(1):7-22.